RSC Advances

ROYAL SOCIETY OF CHEMISTRY

www.rsc.org/advances

Phosphotungstic acid embedded sulfonated poly(arylene ether ketone sulfone) copolymers with amino groups for proton exchange membranes

Lishuang Xu[a], Hailan Han[a], Meiyu Liu[b], Jingmei Xu[a], Hongzhe Ni[a], Hailong Zhang[a], Da Xu[a], Zhe Wang[a,b*]

([a]College of Chemical Engineering, Changchun University of Technology, Changchun 130012, People's Republic of China;

[b]Advanced Institute of Materials Science, Changchun University of Technology, Changchun 130012, People's Republic of China)

Abstract

Sulfonated poly(arylene ether ketone sulfone) containing pendant amino groups (*Am*-SPAEKS)/phosphotungstic acid (HPW) composite membranes with different HPW content were prepared by the solution blend method as proton exchange membrane (PEM) for proton exchange membrane fuel cells (PEMFCs) operation at medium-high temperature. *Am*-SPAEKS were synthesized successfully by adjusting the molar ratio of feeding, which were confirmed by the Fourier transform infrared (FT-IR) spectra and ^{1}H NMR spectra. FT-IR showed that there was acid-base interaction between the amino groups and HPW, as well as HPW and the sulfonic groups. These interactions could stabilized HPW in composite membranes which was confirmed by SEM images. The water uptake and thermal stability of the composite

* Corresponding author. Tel.: 86 431 85716155; fax: 86 431 85716155.
E-mail address: wzccut@126.com (Z. Wang)

membranes were improved compared with the *Am*-SPAEKS membranes. The water retention capacity and the mechanical property of the composite membranes also met the requirement of proton exchange membranes. The proton conductivity of the *Am*-SPAEKS/HPW30% composite membranes reached to 0.091 S cm^{-1} at 120 °C. These results indicated that the *Am*-SPAEKS/HPW composite membranes had potential to be used as alternative proton exchange membrane materials for proton exchange membranes fuel cells at medium-high temperature conditions.

Keywords composite membranes, amino groups, sulfonic groups, HPW, proton conductivity, medium-high temperature

Introduction

Proton exchange membrane fuel cells are popular as energy conversion devices with high energy conversion efficiency, high power density and low pollution, which accomplish the conversion from the chemical energy of fuels to electricity with low greenhouse gas emission. These make them possible to replace other energies applied in portable electronics and vehicles [1-6]. Especially, the operation of PEMFCs has many advantages at moderate-high temperature, such as the simple system design, fast electrode kinetics, reduced water management, high tolerance towards impurities (such as CO) and lower cost, *ect* [7, 8].

Proton exchange membranes not only transfer protons but also isolate the oxidant and fuel as the key components of PEMFCs [9]. The commercially available PEMs for PEMFCs (*e.g*, Nafion®) have high proton conductivity because of the proton transport channel formed by the phase separation between the hydrophilic

groups and the hydrophobic domains below 80 °C [10]. However, the proton conductivity sharply decreases above 80 °C due to the severe water loss.

Therefore, the development of PEMs for medium-high temperature became a research focus. Several strategies have been adopted to achieve high proton conductivity at medium-high temperature and low relative humidity. Such as incorporating inorganic fillers into polymer matrix as hydroscopic agents (TiO_2, SiO_2, ZrO_2) [11-17]. The water uptake of these composite membranes increased due to numerous hydrogen bond sites of these inorganic fillers. However, the composite membranes exhibited relative low proton conductivity because of low intrinsic proton conductivity of these inorganic fillers. [15]. Moreover, these hybrid membranes always displayed poor interfacial connection between organics and inorganics resulting from the weak interactions between inorganic fillers and polymer membranes matrix, which led to the swelling ratio of the membranes increased and then influenced on the dimensional stability of the membranes [18].

A kind of inorganic fillers which possesses the capacity of proton conductivity itself is needed. Phosphotungstic acid ($H_3PW_{12}O_{40}$ abbreviated as HPW) as a solid heteropolyacids attract much interest [19]. It is well known as proton conductors because of its unique Keggin structure [20]. Many attempts at HPW have been made to develop new composite membranes for improving proton conductivity. Ramani *et al*. embedded HPW into Nafion® to prepare the composite membranes, the improvement of conductivity was need to reduce the additive particles sizes, and the proton conductivity of the composite membranes at 120 °C and 35% relative humidity were

on the order of 0.015 S cm^{-1} [21]. Zhou *et al*. used inorganic phosphotungstic acid as proton carrier and mesoporous silica as matrix (HPW-*meso*-silica) developing a new PEM. The proton conductivity was 0.11 S cm^{-1} at 90 °C and 100% relative humidity [22]. Zeng *et al*. fabricated a series of short stacks with 2-cell, 6-cell, 10-cell employing HPW functionalized mesoporous silica PEMs for high temperature with a maximum power density of 74.4 W occurs at 150 °C in H_2/O_2 [23]. Tang *et al*. also developed HPW functionalized mesoporous silica composite membranes by one-step self-assembly route which had a high proton conductivity of 0.06–0.08 S cm^{-1} at 70–100 °C [24]. And Liu *et al* prepared HPW functionalized mesoporous silica by cost-effective tape-casting incorporating phase inversion and vacuum assisted wet impregnation techniques [25]. However, HPW is soluble in water, it is a challenge to immobilize HPW to create a new PEM material with high proton conductivity both at low relative humility and high relative humility, in spite of the proton conductivity of HPW as high as 0.02–0.1 S cm^{-1} at room temperature [26-28]. A new approach was found to immobilize HPW by amino groups, which took advantage of the overall negative charge of the heteropolyanions [29].

On the basis of using sulfonated poly(arylene ether ketone sulfone) containing pendant amino groups (*Am*-SPAEKS), we developed a new medium-high temperature composite PEM with HPW. The N atom on the *Am*-SPAEKS acted as both proton donor and receptor [30, 31]. Thus, they provided a new proton transport channel at medium-high temperature. Particularly, the acid-base interaction between HPW and amino groups was utilized to immobilize HPW to maintain a high proton conductivity

at medium-high temperature. The interaction between sulfonic acid groups and amino groups not only could play a role in immobilizing HPW, but also enhancing the water retention capacity and mechanical properties, improving the dimensional stability and reducing the methanol permeability coefficient of the PEMs.

Experimental

Material

3.3′-disulfonated 4.4′-dichlorodiphenyl sulfone (SDCDPS, 99%), and 4-aminophenyl hydroquinone (4Am-PH, 99%) were synthesized in-house [32, 33]. Tetramethylenesulfone (TMS, CP grade), 2. 2-bis (4-hydroxypheny) propane (bisphenol A, AR grade), and potassium carbonate (K_2CO_3) (AR grade) were purchased from Tianjin XingFu Fine Chemical Industry Research Institute, China. Toluene (AR grade) and HCl (AR grade) were obtained from Beijing Chemical plant, and *N*-methyl-2-pyrrolidinone (NMP, AR grade) was purchased from Tianjin Fu Chen Chemical Reagent Factory, China. HPW were provided by Aladdin Industrial Co (AR grade). 4,4′-Difluorobenzophenone (DFB, AR grade) was obtained from YanBian Long Jing Chemical Company, China, and the solid reagents were used after drying for 12 h at 60 °C under vacuum.

Synthesis of *Am*-SPAEKS

The *Am*-SPAEKS (DS=80%) are synthesized by adjusting the mole ratio of SDCDPS and DFB as shown in Scheme 1. The content of the amino groups for *Am*-SPAEKS is controlled by the mole ratio between 4Am-PH to bisphenol A (2:8).

The direct polycondensation reaction of *Am*-SPAEKS is carried out as followed: DFB (9.0 mmol), bisphenol A (12 mmol), SDCDPS (6.0 mmol), 4Am-PH (3.0 mmol), K_2CO_3 (15 mmol), TMS (16 mL), and toluene (15 mL) were placed into a 100 mL three-neck round-bottom flask equipped with a heating jacket , reflux condenser and a nitrogen inlet. The mixture was refluxed at 130 °C for 4 h with stirring to remove the water produced in reaction by azeotropic distillation. Next, toluene was removed, and the temperature of the reaction mixture was raised to 175 °C and maintained at 175 °C for several hours. When the system viscosity was high enough, heating was stopped, and the solution was poured into a beaker containing deionized water. The obtained strip copolymer was cut into pieces and collected after washed with boiling deionized water to remove solvents and inorganic water-soluble salts, and then dried in a vacuum to obtain the product (in the sodium form). Next, the salt copolymer was immersed in 2 M HCl for 48 h to transform into the acid copolymer, washed with deionized water to remove excess HCl, and dried at 80 °C for 24 h to use.

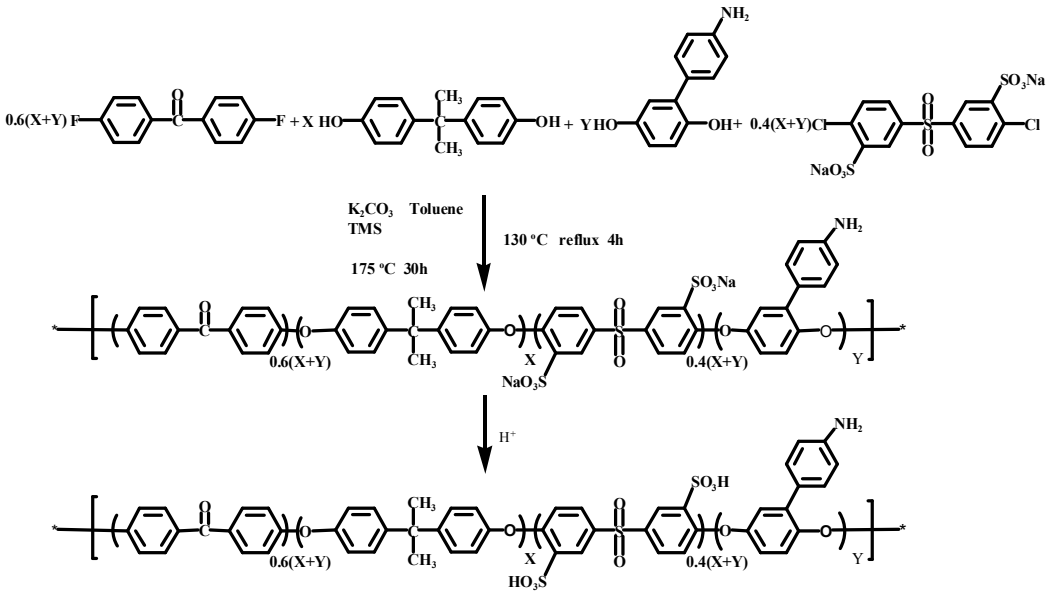

Scheme 1 Synthesis route of *Am*-SPAKES copolymer

Membranes preparation

A series of composite membranes with different content of HPW were prepared and named as *Am*-SPAEKS, *Am*-SPAEKS/HPW10%, *Am*-SPAEKS/HPW20%, *Am*-SPAEKS/HPW30%, respectively. And membrane thickness was at the range of 60-80 μm. Take the preparation of *Am*-SPAEKS/HPW10% for example, the procedure was followed: the acid copolymer (0.9 g) and HPW (0.1 g) were dissolved in 10 mL NMP with stirring and heating to form a homogeneous solution. Next, the solution was poured on the clean and dry glass pane and dried in vacuum oven at 60 °C for 48 h to remove the solvent, and obtained the composite membranes.

Characterization

The ^{1}H NMR spectra were recorded using a Bruker Avance spectrometer with deuterated dimethyl sulfoxide (DMSO-d_6) as the solvent and tetramethylsilane as the internal standard. FT-IR spectroscopy were used to characterize the structures of the samples by using a Vector-22 spectrometer (Bruker, Germany) in the spectral range of 4000–500 cm^{-1}. The thermal stability of the membranes was conducted by thermogravimetric analysis (TGA) using a Perkin Elmer Pyris 1 thermal analyzer under nitrogen atmosphere in the temperature range 50–600 °C at a heating rate of 10 °C min^{-1}. The microstructure of the membranes were recorded by a JSM6510 scanning electron microscope (SEM).

Measurements

Mechanical property

The mechanical property of the membranes were measured on Instron 5965 equipment, and the samples were cut into a dumbbell (25 × 4 mm^2) with fixed between the testing instrument at a tensile rate of 1 mm min^{-1}.

Stability of HPW in the membranes, water uptake and swelling ratio

The prepared membranes were immersed in deionized water at 20 °C for 40 days and dried. The weight loss of HPW were calculated according to the followed formula [34]:

$$Weight\ loss(\%) = \frac{W_{dry1} - W_{dry2}}{W_{HPW}} \times 100\% \qquad (1)$$

Where, W_{HPW} was the weight of HPW initially added, and $W_{dry\ 1}$ and $W_{dry\ 2}$ were the dry weights of the membranes before and after immersed in water, respectively.

The water uptake (WU) of the membranes was measured after the test of stability of HPW in the membranes, and determined by the change in their weights between the dry and the wet membranes. The detailed procedure was reported [33]. The WU was calculated by the followed formula:

$$Water\ Uptake\ (\%) = \frac{W_{wet} - W_{dry}}{W_{dry}} \times 100\% \qquad (2)$$

Where, W_{wet} and W_{dry} were the weight of the wet and the dry membranes, respectively.

The test of the swelling ratio (SR) for the membranes was similar to the WU, but determined by the change in the lengths and the thickness between the wet and the dry membranes. The SR was calculated according to the following formula:

$$Swelling\ ratio\ (\%) = \frac{h_{wet} - h_{dry}}{h_{dry}} \times 100\%$$

$$Swelling\ ratio\ (\%) = \frac{l_{wet} - l_{dry}}{l_{dry}} \times 100\% \quad (3)$$

Where, h_{wet} and h_{dry} were the lengths of dry and wet samples, respectively, then l_{wet} and l_{dry} were the thickness of wet and dry samples.

Water desorption coefficient of the membrane

The water desorption curves represented the water retention capacity of the membranes. And they were reflected by the change weight of water in the membranes with time at a certain temperature. TGA was used to record the water desorption curves at 80 °C for 1 h. The initial stage of the curves obeys the Ficker diffusion laws [31]. The water desorption coefficient was calculated by the following formula:

$$\frac{M_t}{M_\infty} = 4\left(\frac{D_t}{\pi L^2}\right)^{1/2} \quad (4)$$

Where, D_t is the water desorption coefficient of the membrane, M_t/M_∞ is the weight change of the water with time, and L is the width of the membrane.

Oxidative stability

The oxidative stability of the membranes was characterized by the residual weight after immersed in Fenton's reagent (3% H_2O_2, 2 ppm $FeSO_4$) at 80 °C for 1 h. The oxidative stability was evaluated from the percentage of remaining weight of total weight.

Proton conductivity

The membranes (40 mm ×10 mm) were placed in the constant temperature and proton conductivity of the membranes were performed by a four-electrode AC

impedance method at a frequency range of 100 kHz to 0.1 Hz, 10 mV ac perturbation, and 0.0 V dc rest voltage using a Princeton Applied Research Model 2273A Potentiostat (Model 5210 frequency response detector, EG&G PARC, Princeton, NJ) [32]. Before the test, the membranes were immersed in water for 24 h to obtain the 100% relative humidity (RH). Next, the samples were sandwiched between molds, and the temperature was controlled using a constant temperature chamber. The proton conductivity (σ) was calculated by the following equation:

$$\sigma = L/(R \times S) \quad (5)$$

where L (cm) is the distance between the two electrodes, R (Ω) is the membrane resistance, and S (cm^2) is the cross-sectional area of the membrane.

Methanol permeability

The methanol permeability coefficient of the membranes was tested using a custom iron diffusion device, which contained two cells, one was filled with 190 mL methanol solution (10 M), the other one was full of 190 mL pure water, and they were separated by the membranes. The solution of two diffusion cells were magnetically stirred at different temperatures. And the methanol concentration in the water reservoir was measured by a Shimadzu GC-8A chromatograph. The methanol permeability coefficient of the membranes at 25 °C and 60 °C was calculated by following formula [32]:

$$C_{B(t)} = \frac{A}{V_B}\frac{DK}{L}C_A(t - t_0) \quad (6)$$

where C_A and $C_{B(t)}$ (mol m^{-3}) are the methanol concentrations in the methanol and

water reservoirs, respectively; A (cm^2) is the effective area; DK (cm^{-2} s^{-1}) and V_B (mL) are the methanol diffusion coefficient and volume of permeated reservoirs, respectively; L (cm) is the thickness of the membranes.

Results and discussion

The characterization of *Am*-SPAEKS copolymer.

The structures of the copolymers were characterized by their ^{1}H NMR spectrum and FT-IR spectrum. Fig. 1 (a) shows the ^{1}H NMR spectrum of the copolymer. The bond from δ 6.5 to 8.5 ppm are assigned to the protons on the benzene rings of *Am*-SPAEKS as shown in Fig. 1 (a), which is consistent with that reported in the literatures [31, 33]. Thus, the *Am*-SPAEKS are synthesized successfully as shown by the ^{1}H NMR spectrum.

Fig. 1 (b) was the FT-IR spectra of the copolymer. The absorption bands centered at 1231 cm^{-1} and 1095 cm^{-1} can be assigned to the O=S=O and S=O stretching vibrations of sulfonic groups in the FT-IR spectrum of *Am*-SPAEKS membrane, while the peaks at 1162 cm^{-1} can be attributed to the C–S–O bonds. The peaks of N−H stretching vibration appeared at 3458 cm^{-1} and 3352 cm^{-1}. This result further confirmed that the target copolymer was synthesized.

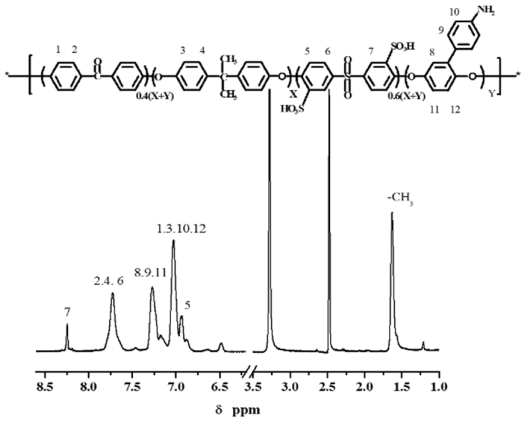

(a)

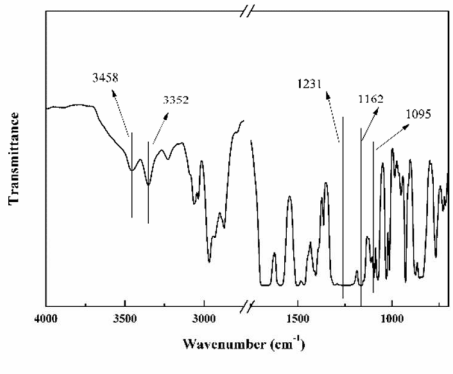

(b)

Fig. 1 The characterization of *Am*-SPAEKS copolymer

FT-IR characterization of HPW, the Am-SPAEKS and Am-SPAEKS/HPW membranes

The FT-IR spectra of HPW, the *Am*-SPAEKS and *Am*-SPAEKS/HPW membranes are shown in Fig. 2. The characteristic peaks of P–O, W=O_t, W–O_c–W, and W–O_e–W stretching vibrations of HPW can be attributed to 1071, 973, 895 and 768 cm^{-1}, respectively, consistent with those reported in the literature for the $[PW_{12}O_{40}]^{3-}$ Keggin unit [35, 36]. The IR absorption cm^{-1}s at 3458 cm^{-1} and 3352 cm^{-1}

are attributed to N−H stretching vibration, while they shift to 3469 cm^{-1} and 3381 cm^{-1} in the IR spectra of the *Am*-SPAEKS/HPW composite membranes. And the characteristic peaks of the sulfonic groups also shift to 1235 cm^{-1} and 1097 cm^{-1}. In addition, the absorption peaks of HPW shift from 1071, 973 and 895 cm^{-1} to 1079, 980 and 893 cm^{-1}. This demonstrates that there are the strong hydrogen-bonding interactions between the sulfonic groups and HPW, and the acid-base interaction between the amino groups and HPW. These results indicated the *Am*-SPAEKS/HPW composite membranes were prepared successfully.

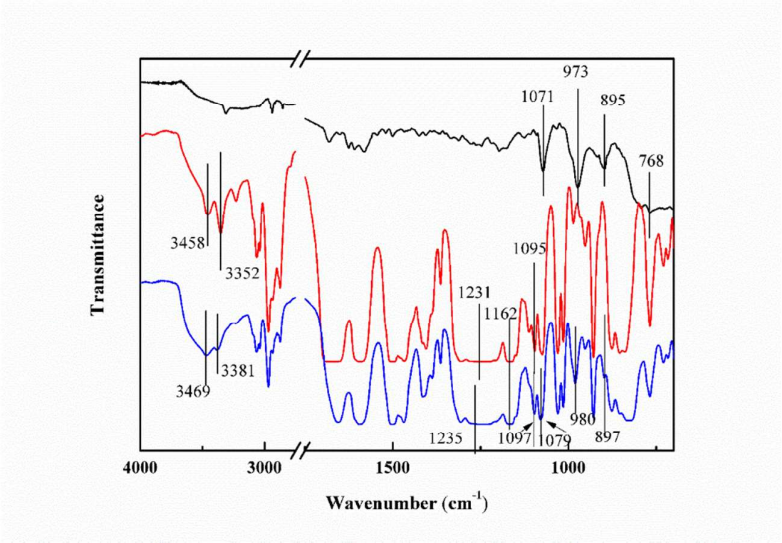

Fig. 2 FT-IR spectra of HPW, *Am*-SPAEKS and *Am*-SPAEKS/HPW.

Thermal and mechanical performance of the membranes

The thermal properties of the membranes was performed using TGA by recording the weight loss of the membranes with temperature. The TGA curves of the membranes were shown in Fig. 3. The *Am*-SPAEKS membranes showed three weight loss steps. First step around 100 °C is due to the evaporation of residual solvent and water molecules. Second step around 200 °C corresponds to the degradation of the

sulfonic groups from copolymers. The last step started around 400 °C which is attributed to the decomposition of the polymer main chain. The composite membranes present similar decomposition patterns, but the temperature at which the sulfonic acid groups degraded is higher than that of the *Am*-SPAEKS membranes. This can be explained by that HPW had excellent thermal stability as shown in Fig.3 and the interaction between the sulfonic groups and HPW improved the stability of the sulfonic groups. This result demonstrated that the composite membranes exhibited favorable thermal properties.

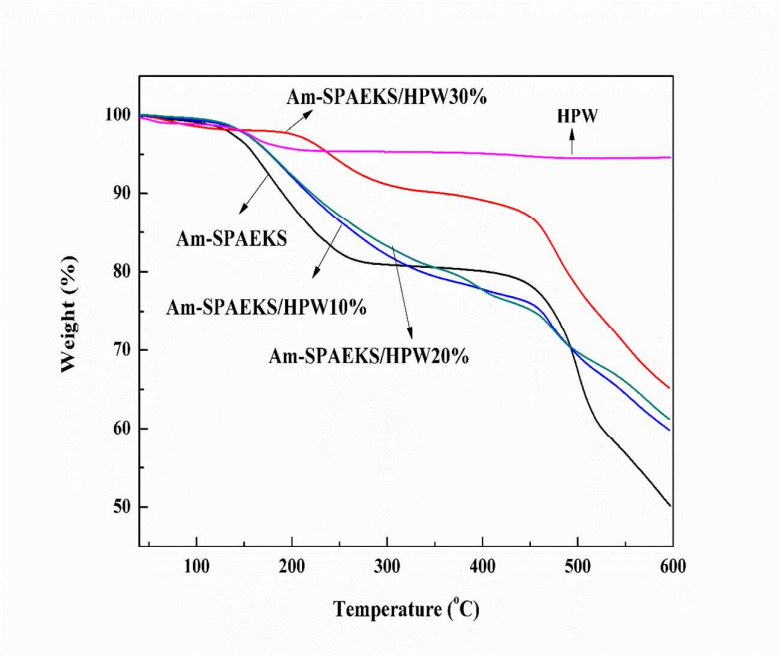

Fig. 3 TGA curves of the membranes and HPW.

PEMs is requested to possess good tensile strength in the application of PEMFCs. In Table 1, the mechanical properties of the membranes were listed. With increasing the HPW, The Young's Modulus and the tensile strength of the composite membranes decreased because of reduced content of *Am*-SPAEKS, which acted as network in the membranes. Thus, the stretch of the backbone was restricted and hindering the strain

[25]. But the Young's Modulus and the tensile strength of the composite membranes can also reach at 1392.76 MPa and 38.29 MPa, respectively. This shows that the composite membranes possesses appropriate mechanical performance to meet the requirements of PEMs.

Table 1 $T_{d5\%}$[a], oxidative stability and mechanical properties of membranes

Samples	$T_{d5\%}$ (°C)	Oxidative stability (%) 80 °C	Young's Modulus (MPa) 25 °C	Tensile strength (MPa) 25 °C
Nafion®	-	98	186	36.64
Am-SPAEKS	162	94.74	1765.76	62.17
Am-SPAEKS/HPW10%	182	93.18	1702.15	59.19
Am-SPAEKS/HPW20%	185	90.48	1594.61	39.30
Am-SPAEKS/HPW30%	242	88.75	1392.76	38.29

[a]$T_{d5\%}$ is the temperature when weights of membranes lost 5%.

Morphology

The morphology have a direct impact on the performances of the membranes. The microstructure of membranes were observed by SEM. As shown in Fig. 4, the *Am*-SPAEKS membranes was smooth and compact which favorable mechanical property and thermal stability based on. The white part is HPW particles in the images of composite membranes. It can be found that HPW particles disperse evenly from the cross-sectional and surface morphology of composite membranes which results from not only the interaction between amino groups and HPW, but also the interaction between the sulfonic groups and HPW. In addition, with increasing HPW, the white parts became more and intensive. This indicated that HPW particles dispersed evenly in composite membranes.

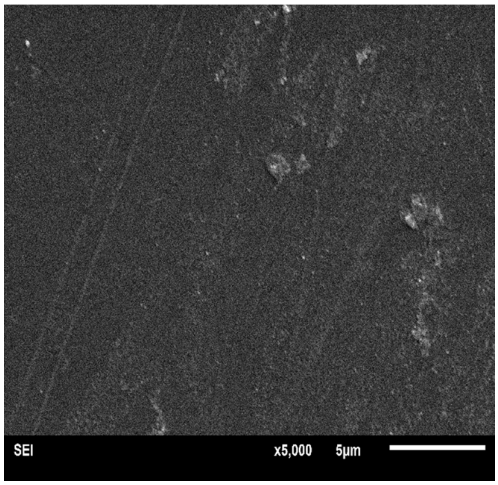

(a) surface of *Am*-SPAEKS

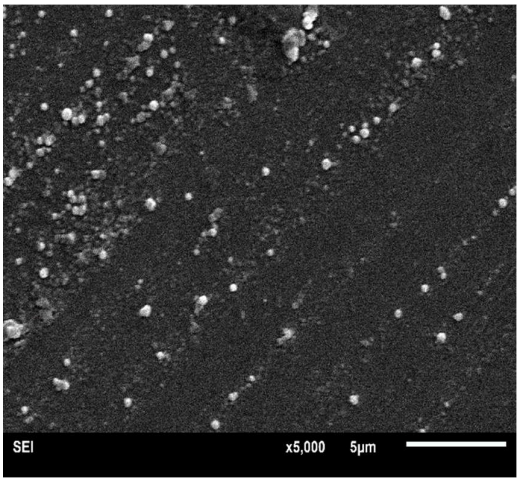

(b) surface of *Am*-SPAEKS/HPW10%

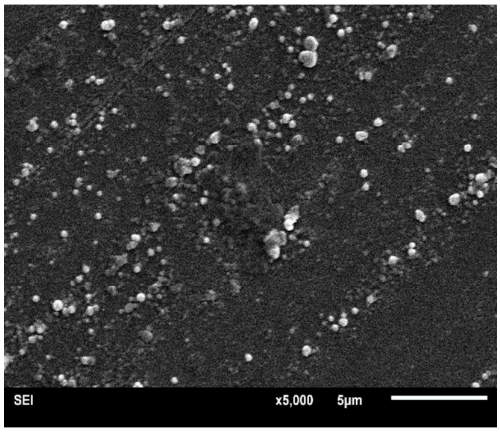

(c) surface of *Am*-SPAEKS/HPW20%

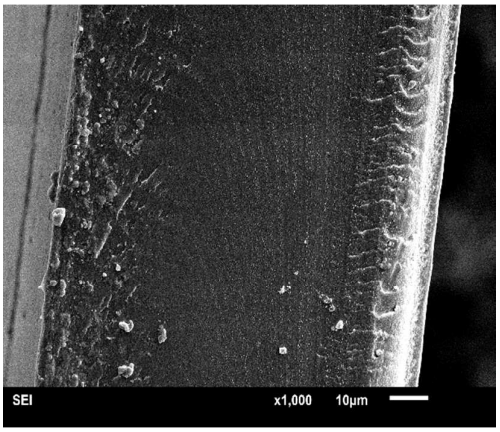

(d) cross-sectional morphology of *Am*-SPAEKS/HPW30%

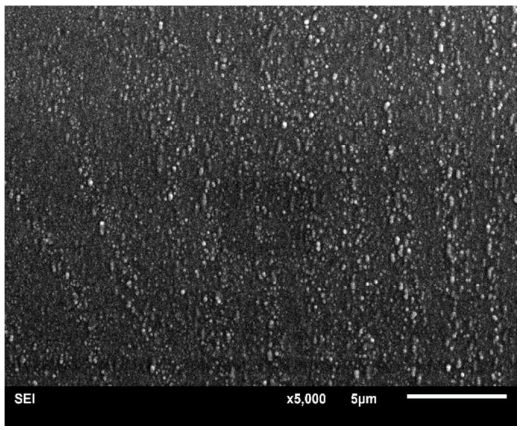

(e) cross-sectional morphology of *Am*-SPAEKS/HPW30%

Fig. 4 SEM images of *Am*-SPAEKS and *Am*-SPAEKS/HPW membranes

Stability of HPW in the membranes, water uptake and swelling ratio

The stability of HPW in the membranes was evaluated by the weight loss of HPW in the composite membranes after immersed in water at 25 °C for 40 days. The HPW release was calculated and displayed in Table 2. The release ratio of HPW increases from 8.3% to 13.9% with increasing HPW content, but remains a low level as expected. It could be explained by the interaction between HPW and amino groups as well as the acid-base interaction between sulfonic groups and amino groups. The acid-base interaction between amino groups and HPW stabilized HPW particles, and the acid-base interaction between sulfonic groups and amino groups formed network to surround the HPW particles. Besides, the hydrogen bond interaction (between sulfonic groups and HPW) immobilized HPW further in the membranes.

The efficient water uptake is necessary for electrolyte membranes to transfer protons because that water is treated as the proton carrier, and protons are transferred in PEMs through forming hydrated protons with water molecules (H_3O^+ and $H_5O_2^+$) [37]. The water uptake of the membranes at different temperature are shown in Fig. 5. The uptakes of the *Am*-SPAEKS/HPW composite membranes increase with increasing HPW. The maximum WU of the *Am*-SPAEKS/HPW30% membranes could reach at 22.58% at 80 °C. This is due to that the HPW acts as a conductor and facilitates H_2O molecules to permeate into the membranes, and HPW is highly hydrophilic, it is beneficial to absorb water molecules and increase the WU [38].

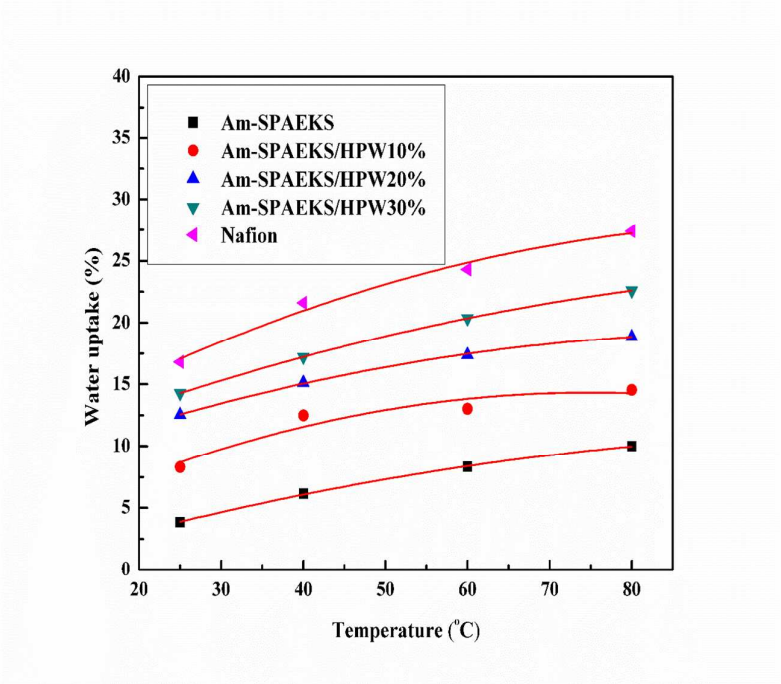

Fig. 5 Water uptake of *Am*-SPAEKS and *Am*-SPAEKS/HPW membranes

Abundant hydration is essential for PEMs to maintain high proton conductivity. However, excess water uptake will cause extreme swelling ratio leading to the decline of the mechanical performance and dimensional stability [33]. Thus, a moderate swelling ratio is also critical which is beneficial to prevent fuel from permeating through PEMs. Fig. 6 shows the swelling ratio of the membranes. It can be found that the swelling ratio of composite membranes is higher than that of *Am*-SPAEKS membranes. This is explained by that the interaction between the amino groups and the sulfonic acid groups is weakened by the addition of HPW, which results in increasing the free volume of the composite membranes leading to increasing swelling ratio, compared with *Am*-SPAEKS membranes. But the swelling ratios of composite membranes are also enough to meet the requirement for PEMs (the swelling ratio of Nafion® was 27% at 80 °C).

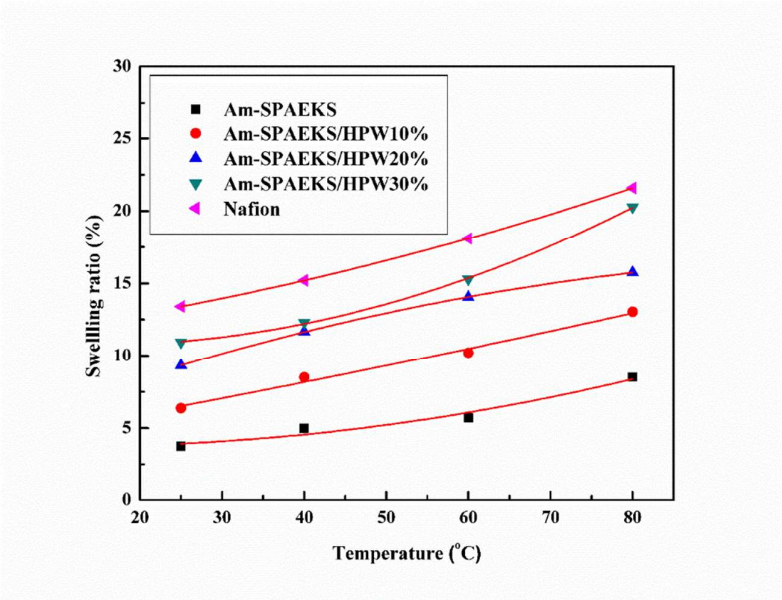

Fig. 6 Swelling ratio of *Am*-SPAEKS and *Am*-SPAEKS/HPW membranes

Water retention capacity

The water retention capacity of PEMs plays an important role on proton conductivity because that PEMs transfer protons among sulfonic acid groups by the formation and cleavage of the hydrogen bond network by water molecules. Fig. 7 shows the water absorption curves which are obtained by recording the weight loss of the membranes using TGA at 80 °C for 1 h. The water diffusion coefficients are listed in Table 2. The lower water diffusion coefficients indicates better water retention capacity, while the higher water diffusion coefficients indicates the worse water retention capacity. The water diffusion coefficients of the composite membranes are lower (the maximum water diffusion coefficients 4.2 $\times 10^{-8}$ cm^2 s^{-1}) than that of *Am*-SPAEKS (9.1 $\times 10^{-8}$ cm^2 s^{-1}), and they decrease with increasing HPW. This is because that the acid-base interaction between the amino groups and the sulfonic groups could form network to prevent water molecules from moving freely, limiting

the evaporation of water in the composite membranes. Moreover, the HPW was immobilized by the amino groups and the unique structure of the anion can bound water molecules in the composite membranes. The water retention principle of the composite membranes was showed in Scheme 2.

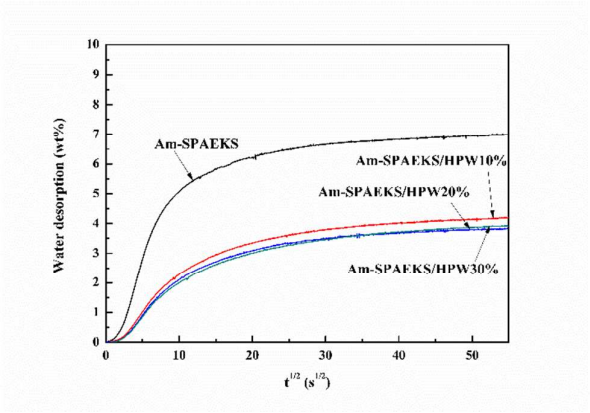

Fig. 7 Water diffusion coefficient of *Am*-SPAEKS and *Am*-SPAEKS/HPW membranes

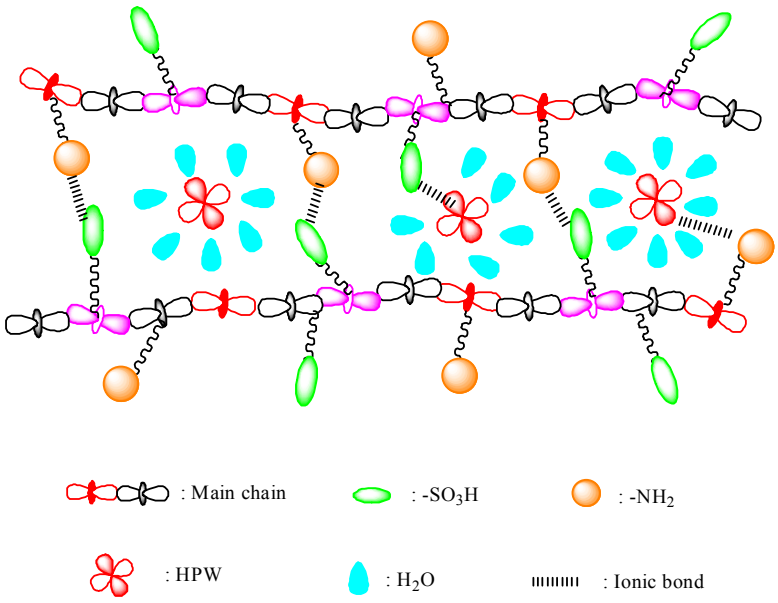

Scheme 2 The water retention principle of the composite membranes

Oxidative stability

The oxidative stability is another important parameter of evaluating the

performance for PEMs. It is determined the residual weight after immersed in Fenton's reagent at 80 °C for 1 h as the test of oxidative stability of the available PEMs Nafion®. The test results of the oxidative stability for the membranes were displayed in Table 1. It can be found that the composite membranes have weaker oxidative stability than that of *Am*-SPAEKS, and with increasing the content of HPW, the oxidative stability declines. This is because that the interaction between HPW and the amino groups stabilized HPW, and HPW is hydrophilic to increase the WU efficiently, the increased water content benefits the transport of peroxides, thus accelerating the degradation [39]. That is why the oxidative stability of the *Am*-SPAEKS/HPW composite membranes (the residual weight from 93.18% to 88.75%) is lower than that of the *Am*-SPAEKS membranes (94.74%). In general, the composite membranes exhibited satisfactory antioxidant stability compared with Nafion® of 98% [40].

Proton conductivity and methanol permeability

Proton conductivity has a significant impact on the performance of PEMs, and PEMs must possess high proton conductivity as the core component of PEMFCs. The proton conductivity of the membranes was shown in Fig. 8. It is observed that proton conductivity of the membranes increased with increasing HPW at the same temperature and relative humidity. This is due to that the special anion structure of HPW can combine hydrated protons to transfer them across the membranes like the sulfonic acid groups [38]. Although the proton conductivity decrease slightly with increasing the test temperature above 80 °C, it is also higher than that of the

Am-SPAEKS membranes and Nafion® (at the range of 0.063-0.018 S cm $^{-1}$ from 80 °C to 120 °C). At low temperature, the protons are transferred according to the "Vehicular" mechanism by HPW and the sulfonic acid groups which is depended on water environment [41] as shown in Scheme 3 (a). Above 80 °C, the protons transfer based on both the "Grotthuss" and "Vehicular" mechanism because of the enhancement of the water retention capacity of the composite membranes, when the protons transmission is accomplished not only by HPW and the sulfonic acid groups as shown in Scheme 3 (a), but also the formation and fracture of the hydrogen bonding between N atoms and HPW as shown in Scheme 3 (b). Thus, the *Am*-SPAEKS/HPW30% composite membranes maintain high proton conductivity from 0.095–0.091 S cm $^{-1}$ in the temperature range of 80 °C to 120 °C.

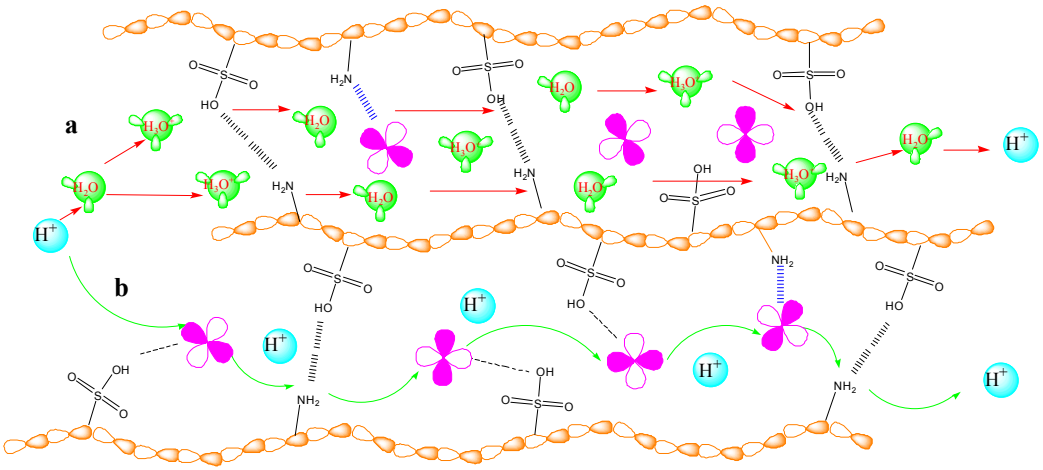

Scheme 3 Illustration of proton transfer mode

The Arrhenius plot of the membranes was shown in Fig. 9. The activation energies of proton transfer for the membranes were calculated by the Arrhenius equation. It is found that the activation energies for the *Am*-SPAEKS, *Am*-SPAEKS/HPW10%, *Am*-SPAEKS/HPW20% and *Am*-SPAEKS/HPW30% are

similar at below 80 °C, this indicates that proton transfer might occur mainly by the water environment [42]. With HPW increasing, the activation energies of the composite membranes decrease, and lower than that of the *Am*-SPAEKS membranes, this phenomenon become obvious from 80 °C to 120 °C (the activation energies of *Am*-SPAEKS to the *Am*-SPAEKS/HPW30% was from 5.7 kJ mol^{-1} to 1.2 kJ mol^{-1}). It means that the composite membranes transported protons more easily than the *Am*-SPAEKS membranes at this range of temperature. This is caused by three aspects: first, the acid-base interaction improve the water retention capacity of the composite membranes, thus maintain low the activation energy; second, the N atoms act as proton donor and acceptor [31], thus shorten the distance of proton transmission and provide a new channel; third, the HPW immobilized by the amino groups, provides more active sites for transmission of protons among the functional groups (amino groups and sulfonic acid groups), which bases on its hydrophilic nature. These factors resulted in the lower activation energy of proton conductivity of the composite membranes than that of the *Am*-SPAEKS membranes from 80 °C to 120 °C.

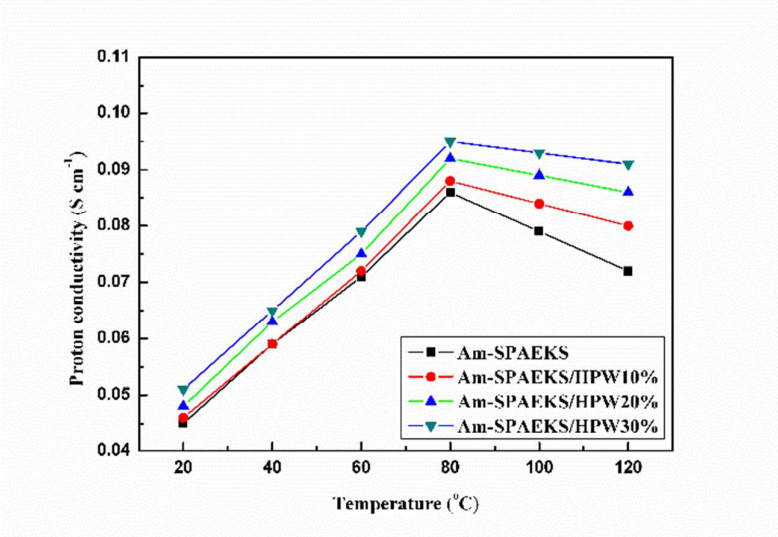

Fig. 8 Proton conductivity of the membranes.

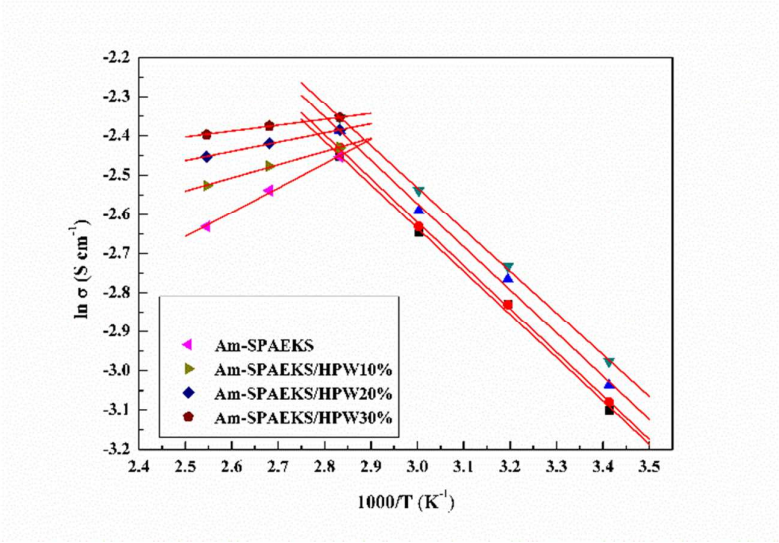

Fig. 9 Arrhenius plot of proton conductivity vs temperature

The proton conductivity at different RH condition was measured to further verify the effect of inorganic materials on the proton transport as shown in Fig. 10. At 100% RH condition, the proton conductivity of all samples were similar. However, with the RH decreasing the composite membranes displayed higher proton conductivity compared to the *Am*-SPAEKS membranes. Moreover, the proton conductivity of the *Am*-SPAEKS membranes dropped significantly at low RH (< 80%). This is due to the following aspects: (i) the composite membranes had better water retention capacity to maintain high proton conductivity at low RH, and (ii) the HPW had intrinsic capacity of transporting protons which played an important role in proton transport at low RH.

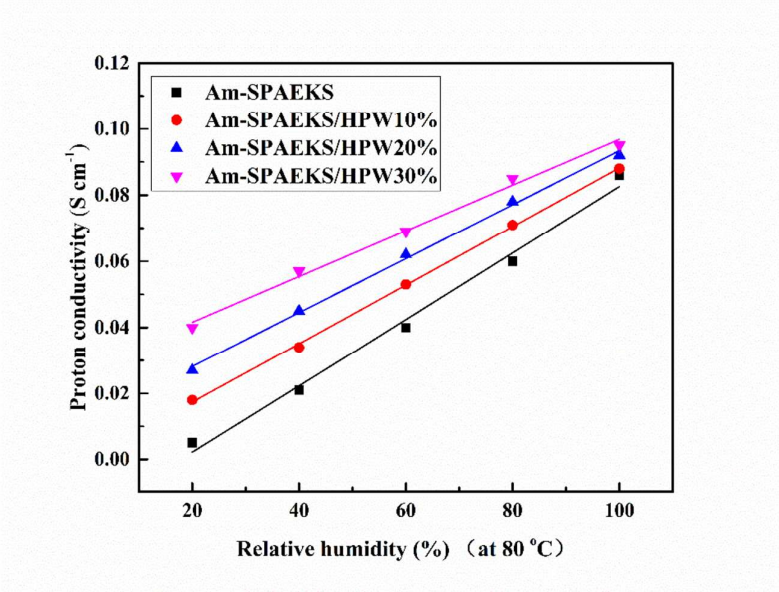

Fig. 10 Proton conductivity of the membranes at different relative humidity

Both hydrogen and methanol were used in the PEMFCs as fuel. Thus, the methanol permeability coefficient of the membranes need to be studied. In this paper, the methanol permeability coefficient of the membranes were investigated by 10 M methanol solution at 25 °C and 60 °C. The results were presented in Table 2. The methanol permeability coefficient of composite membranes are in the range of 10.25 × 10^{-7} cm^2 s^{-1} to 15.83 × 10^{-7} cm^2 s^{-1} at 25 °C, it is found that the methanol permeability coefficient of composite membranes increase with increasing HPW, and higher than that of *Am*-SPAEKS membranes. This might be relative to that the addition of HPW reduce the acid-base interaction between the amino groups and the sulfonic acid groups, widening the free volume absorbed water molecules, leading to a loose structure of composite membranes, inducing higher methanol permeability coefficient. In spite of that, it also displayed low methanol diffusion coefficient.

Table 2 The analytical data of *Am*-SPAEKS and *Am*-SPAEKS/HPW membranes

Samples	HPW release (%)	Methanol diffusion coefficient ($\times10^{-7}$ cm^2 s^{-1}) 25 °C	60 °C	Water diffusion coefficient ($\times10^{-8}$ cm^2 s^{-1}) 80 °C	Ea (kJ mol^{-1}) ≥ 80 °C	Proton conductivity (S cm^{-1}) 80 °C	120 °C
Nafion®	-	24.8	-	-	-	0.063	0.018
Am-SPAEKS	-	8.36	17.13	9.1	5.7	0.086	0.072
Am-SPAEKS/HPW1 0%	8.3	10.25	20.02	4.2	2.8	0.088	0.080
Am-SPAEKS/HPW2 0%	12.5	12.51	22.76	3.9	1.9	0.092	0.086
Am-SPAEKS/HPW3 0%	13.9	15.83	25.34	2.6	1.2	0.095	0.091

Conclusion

In a word, the *Am*-SPAEKS with a certain DS was synthesized by direct polycondensation reactions, the content of the amino groups was constant. The composite membranes were prepared by solution blend method. The FT-IR spectrum indicated that there were acid-base interaction between the amino groups and the sulfonic groups, and between amino groups and HPW, which could immobilized HPW in composite membranes. SEM images showed that HPW dispersed evenly, there was no phase separation. Composite membranes exhibited favorable performance, such as thermal property, dimension stability, oxidative stability and mechanical performance. In particular, the proton conductivity of composite membranes was improved at medium-high temperature.

Acknowledgement

The authors thank the Natural Science Foundation of China (Grant No: 51273024 and 51303015), Department of Education of Jilin Province (Grant No: 2014119), and the Scientific and Technological Planning Projects of the Jilin Province

(Grant No. 20130101021JC) for the financial support for this study.

References

1. M. Z. Jacobson, W. G. Colella and D. M. Golden, *Science*, 2005, **308**, 1901-1905.

2. M. Nogami, H. Matsushita, Y. Goto and T. Kasuga, *Adv. Mater.*, 2000, **12**, 1370-1372.

3. P. Agnolucci, *Int. J. Hydrogen Energy*, 2007, **32**, 4306-4318.

4. P. Costamagna and S. Srinivasan, *J. Power Sources*, 2001, **102**, 253-269.

5. S. P. Jiang, Z. Liu and Z. Q. Tian, *Adv. Mater.*, 2006, **18**, 1068-1072.

6. Y. Yang, H. Gao and L. Zheng, *RSC Adv.*, 2015, **5**, 17683-17689.

7. L. Cindrella, A. M. Kannan, J. F. Lin, K. Saminathan, Y. Ho, C. W. Lin and J. Wertz, *J. Power Sources*, 2009, **194**, 146-160.

8. A. M. Kannan, L. Cindrella and L. Munukutla, *Electrochim. Acta*, 2008, **53**, 2416-2422.

9. X. Xu, L. Li, H. Wang, X. Li and X. Zhuang, *RSC Adv.*, 2015, **5**, 4934-4940.

10. C. Zhao, D. He, Y. Li, J. Xiang, P. Li and H.-J. Sue, *RSC Adv.*, 2015, **5**, 47284-47293.

11. A. Saccà, A. Carbone, E. Passalacqua, A. D'Epifanio, S. Licoccia, E. Traversa, E. Sala, F. Traini and R. Ornelas, *J. Power Sources*, 2005, **152**, 16-21.

12. A. K. Sahu, G. Selvarani, S. Pitchumani, P. Sridhar and A. K. Shukla, *J. Electrochem. Soc.*, 2007, **154**, B123-B132.

13. A. Saccà, I. Gatto, A. Carbone, R. Pedicini and E. Passalacqua, *J. Power Sources*, 2006, **163**, 47-51.

14. C. H. Rhee, H. K. Kim, H. Chang and J. S. Lee, *Chem. Mater.*, 2005, **17**, 1691-1697.

15. H. M. L. Thijs, C. R. Becer, C. Guerrero-Sanchez, D. Fournier, R. Hoogenboom and U. S. Schubert, *J. Mater. Chem.*, 2007, **17**, 4864-4871.

16. A. M. Herring, *J. Macromol. Sci., Part C*, 2006, **46**, 245-296.

17. E. A. Mistri and S. Banerjee, *RSC Adv.*, 2014, **4**, 22398-22410.

18. S. S. Kulkarni, S. M. Tambe, A. A. Kittur and M. Y. Kariduraganavar, *J. Membr. Sci.*, 2006, **285**, 420-431.

19. S. V. Sambasivarao, Y. Liu, J. L. Horan, S. Seifert, A. M. Herring and C. M. Maupin, *J. Phys. Chem. C*, 2014, **118**, 20193-20202.

20. V. Ramani, H. R. Kunz and J. M. Fenton, *J. Membr. Sci.*, 2005, **266**, 110-114.

21. V. Ramani, H. R. Kunz and J. M. Fenton, *J. Membr. Sci.*, 2004, **232**, 31-44.

22. Y. Zhou, J. Yang, H. Su, J. Zeng, S. P. Jiang and W. A. Goddard, *J. Am. Chem. Soc.*, 2014, **136**, 4954-4964.

23. J. Zeng, B. Jin, P. K. Shen, B. He, K. Lamb, R. De Marco and S. P. Jiang, *Int. J. Hydrogen Energy*, 2013, **38**, 12830-12837.

24. H. Tang, M. Pan, S. Lu, J. Lu and S. P. Jiang, *Chem. Commun.*, 2010, **46**, 4351-4353.

25. L. Bai, L. Zhang, H. Q. He, R. K. S. O. A. Rasheed, C. Z. Zhang, O. L. Ding and S. H. Chan, *J. Power Sources*, 2014, **246**, 522-530.

26. C. Pazé, S. Bordiga and A. Zecchina, *Langmuir*, 2000, **16**, 8139-8144.

27. S. Uchida, K. Inumaru and M. Misono, *J. Phys. Chem. B*, 2000, **104**, 8108-8115.

28. E. Fontananova, F. Trotta, J. C. Jansen and E. Drioli, *J. Membr. Sci.*, 2010, **348**, 326-336.

29. G. Luo, L. Kang, M. Zhu and B. Dai, *Fuel Process. Technol.*, 2014, **118**, 20-27.

30. W.-Q. Deng, V. Molinero and W. A. Goddard, *J. Am. Chem. Soc.*, 2004, **126**, 15644-15645.

31. J. Xu, H. Cheng, L. Ma, H. Han, Y. Huang and Z. Wang, *J Polym Res*, 2014, **21**, 1-11.

32. Y. Zhang, Y. Wan, G. Zhang, K. Shao, C. Zhao, H. Li and H. Na, *J.Membr. Sci.*, 2010, **348**, 353-359.

33. H. Cheng, J. Xu, L. Ma, L. Xu, B. Liu, Z. Wang and H. Zhang, *J. Power Sources*, 2014, **260**, 307-316.

34. D. Xu, G. Zhang, N. Zhang, H. Li, Y. Zhang, K. Shao, M. Han, C. M. Lew and H. Na, *J. Mater. Chem.*, 2010, **20**, 9239-9245.

35. B. B. Bardin, S. V. Bordawekar, M. Neurock and R. J. Davis, *J. Phys. Chem. B*, 1998, **102**, 10817-10825.

36. J. Yang, M. J. Janik, D. Ma, A. Zheng, M. Zhang, M. Neurock, R. J. Davis, C. Ye and F. Deng, *ChemInform*, 2006, **37**, no-no.

37. G. Wang, Y. Yao, G. Xiao and D. Yan, *J. Membr. Sci.*, 2013, **425–426**, 200-207.

38. H. T. Li, G. Zhang, J. Wu, C. J. Zhao, Y. Zhang, K. Shao, M. M. Han, H. D. Lin, J. Zhu and H. Na, *J. Power Sources*, 2010, **195**, 6443-6449.

39. H. Wu, X. Shen, Y. Cao, Z. Li and Z. Jiang, *J. Membr. Sci.*, 2014, **451**, 74-84.

40. J. Kim, D. Kim, J. Membr. Sci., 2012, 405-406, 176-184.

41. R. Subbaraman, H. Ghassemi and T. A. Zawodzinski, *J. Am. Chem. Soc.*, 2007, **129**, 2238-2239.

42. Q. Zhang, S. Zhang and S. Li, *Int. J. Hydrogen Energy*, 2011, **36**, 5512-5520.